Synthesis and characterization of Co doped magnetoelectric $Bi_2Fe_4O_9$

A thesis submitted in partial fulfillment for the award of degree in

Master of Science
In
Physics

By

Ms.Smita Swain

Roll No.411PH2120

Under Guidance of

Dr. Anil K. Singh

Department of Physics

National Institute Of Technology, Rourkela
Rourkela- 769008, Odisha, India
Academic year: 2011-2013

DECLARATION

I hereby declare that the work carried out me at Department of Physics, National Institute of Technology, Rourkela. I further declare that to best of my knowledge the carried out experimental work has not formed the basis for the award of any degree, diploma, or similar title of any university or institution.

Date:
Place: Rourkela

Smita Swain
Roll Number: 411PH2120
Department of Physics
National Institute of Technology
Rourkela, 769008

Department of PhysicsNational Institute of Technology RourkelaRourkela-769008Odisha, India

CERTIFICATE

This is to certify that the thesis entitled "**Synthesis and Characterization of Co doped magnetoelectric $Bi_2Fe_4O_9$**" being submitted by **SMITA SWAIN** in partial fulfilment of the requirements for the award of the degree of Master of Science in Physics at National Institute of Technology, Rourkela is an authentic experimental work carried out by her under our supervision. To the best of our knowledge, the experimental matter embodied in the thesis has not been submitted to any other University/Institute for the award of any degree or diploma.

Date:

_____

Dr. Anil K. Singh

Abstract

MultiferroicBi$_2$Fe$_4$O$_9$ and Co doped Bi$_2$Fe$_4$O$_9$ are prepared by solid state route reaction method using bismuth oxide (Bi$_2$O$_3$), iron oxide (Fe$_2$O$_3$) and cobalt oxide (Co$_3$O$_4$). X-ray diffraction (XRD) results confirm that there is no change in crystal structure due to Co doping. Scanning Electron Microscopy image shows grain size increases due to doping which is in agreement with XRD analysis. From dielectric constant measurement we conclude that dielectric constant increases due to Co doping. UV-Visible plot shows due to Co doping band gap energy increases.

Index

1. INTRODUCTION

1.1. MAGNETIC MATERIALS

The materials which can be either attracted or repelled when placed in an external magnetic field and can be magnetised themselves are known as magnetic materials. When a material is placed in a magnetic field, magnetic forces of the material's electrons will be affected. The materials can react quite differently to the presence of an external magnetic field. The reaction is dependent on the atomic and molecular structure of the material, and the net magnetic field associated with the atoms. The magnetic moments associated with atoms have three origins. These are the electron motion, the change in motion caused by an external magnetic field, and the spin of the electrons. The magnetic behaviour of materials can be classified into following groups:

(i) DIMAGNETISM

Diamagnetic substances are composed of atoms which have no net magnetic moments. However exposed to a field a negative magnetization is produced and thus the susceptibility is negative.

Examples: Quartz, calcite, water

(ii) PARAMAGNETISM

This class of materials, some of the atoms or ions in the material have a net magnetic moment due to unpaired electrons. This has positive susceptibility. It obeys curie law.

Examples: Biotite, Siderite, Pyrite

Curie law

In paramagnetic substance magnetic susceptibility is inversely proportional to temperature. Mathematically, $\chi = C/T$, Where C is the curie constant.

(iii) FERROMAGNETISM

These materials have a large, positive susceptibility to an external magnetic field. They exhibit a strong attraction to magnetic fields and are able to retain their magnetic properties after the external field has been removed. They have also some unpaired electrons so their atoms have a net magnetic moment.

Curie-Weiss law

The Curie-Weiss law describes the magnetic susceptibility of a ferromagnet in the paramagnetic region above the Curie point.

Mathematically $\chi = C/ (T-T_C)$

Examples: Iron, nickel and cobalt.

(iv) ANTIFERROMAGNETISM

In materials that exhibit antiferromagnetism the magnetic moments are aligned in opposite directions and are of equal magnitude. These materials are unmagnetised due to zero magnetic moments. After a certain temperature called Nèel temperature it shows paramagnetic behaviour.

Examples: MnO, FeO, CoO, NiO, Cr

***Application of magnetic materials*:**

Power conversion electrical-mechanical, Power adaption, signal transfer, magnetic field screening, bubble memory.

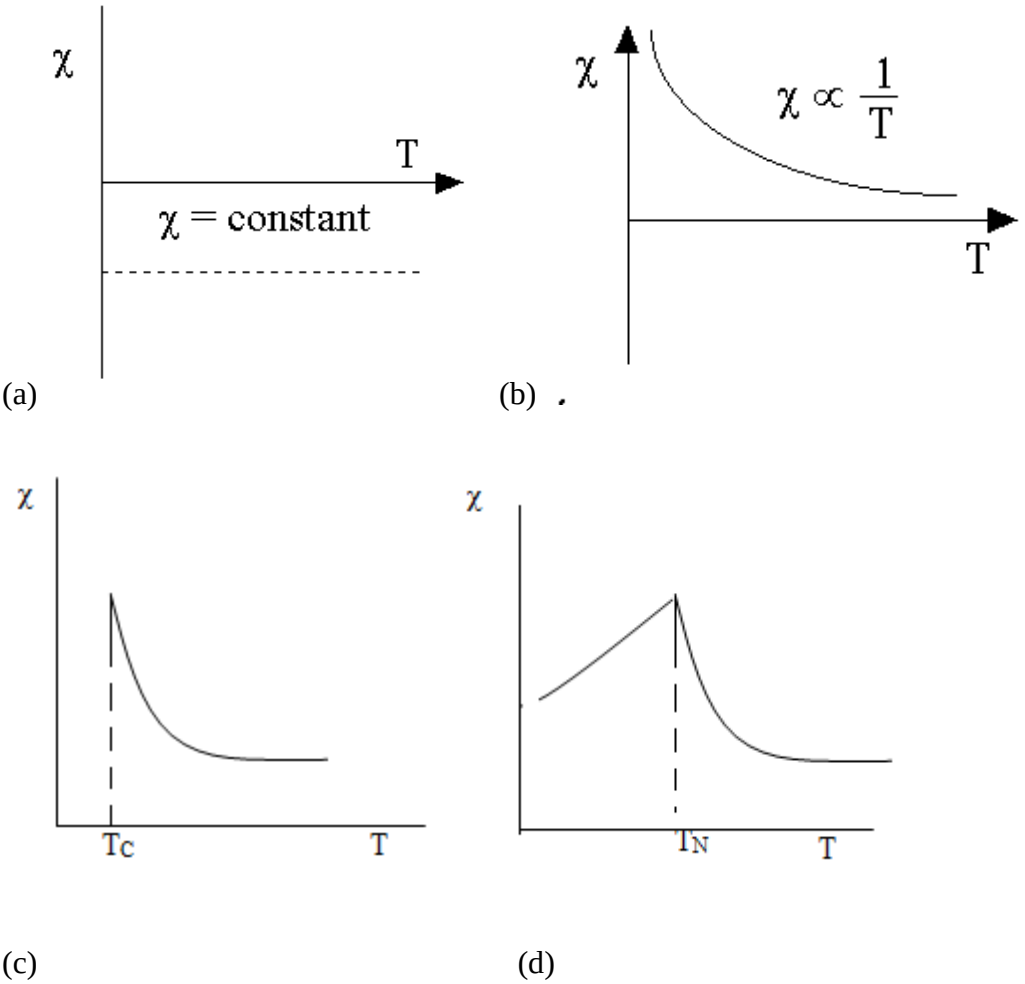

Fig. 1.1- susceptibility versus temperature graph of (a) diamagnetism (b) paramagnetism (c) Ferromagnetism (d) antiferromagnetism.

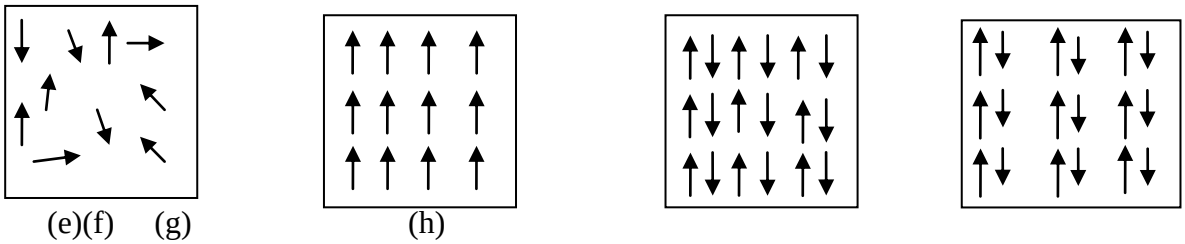

Fig.1.1 -Spin orientation in (e) paramagnetism (f) ferromagnetism (g) antiferromagnetism (h) ferrimagnetism.

1.2. FERROELECTRIC MATERIALS

Ferroelectricity is the effect of spontaneous electric polarization of a material; it can be reversed by application of an electric field. Ferroelectricity was first discovered in Rochelle salt in 1921. A ferroelectric material possesses at least two equilibrium orientations of the spontaneous polarization vector in the absence of an external electric field. The spontaneous polarization can be switched between those orientations by an electric field.

Among the 32 crystal classes, 11 of them are characterized by the existence of a centre of symmetry. The remaining 21 crystal classes do not have a centre of symmetry. Thus it is possible for the 21 groups to have one or more polar axes and possess odd-rank tensor properties. There is an exception that is the group 432 which lacks a centre of symmetry but it has also other symmetry operations that destroy polarity. All non-centrosymmetric point groups exhibit piezoelectric effect which is defined by a change in electric polarity under applied stress. Among the 20 piezoelectric classes, 10 possess a unique polar axis, which spontaneous polarization depends on temperature. This is called pyroelectric effect. All ferroelectric crystals belong to pyroelectric family which has a spontaneous polarization that can be reversed.

Among all ferroelectric materials the most extensively studied and widely used are the perovskite. The perovskite has the general formula ABO_3. Where A represents a divalent or trivalent cation and B is typically a tetravalent or trivalent cation. B must be smaller than A.

Example of perovskites

Let's take an example of $BaTiO_3$. Here the Ba^{2+}cations are located at the corners of the unit cell. A dipole moment occurs due to relative displacements of the Ti and O ions from their symmetrical positions.

Here =A

=O

=B

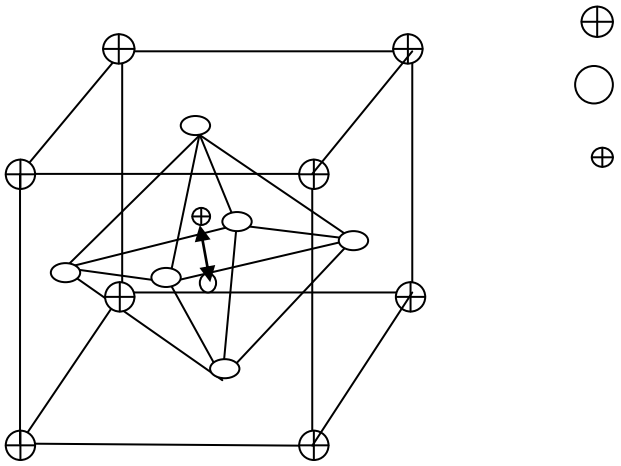

Fig 1.2 - Crystal structure of perovskite ABO_3.

Application of ferroelectric materials:

Used in capacitors, non-volatile memory, light deflectors, modulators and displays, piezoelectric for ultrasound imaging and actuators, oscillators and filters.

1.3. FERROELASTIC MATERIALS

The materials which develop a spontaneous strain below a phase transition temperature are known as ferroelastic materials. A crystal is ferroelastic if it has two or more stable orientation states in the absence of mechanical stress and if it can be reproducibly transformed from one to another of these states by application of mechanical stress.

Examples: Gadolinium molybdate and lead phosphate.

Application of ferroelastic materials:

Used in actuators, sensors

1.4. SPIN FRUSTRATION

In spin frustrated system the last spin does not know how to align. For example consider a triangle system in which we have to arrange the spins in antiferromagnetic order how the spin is frustrated is given by the figure.

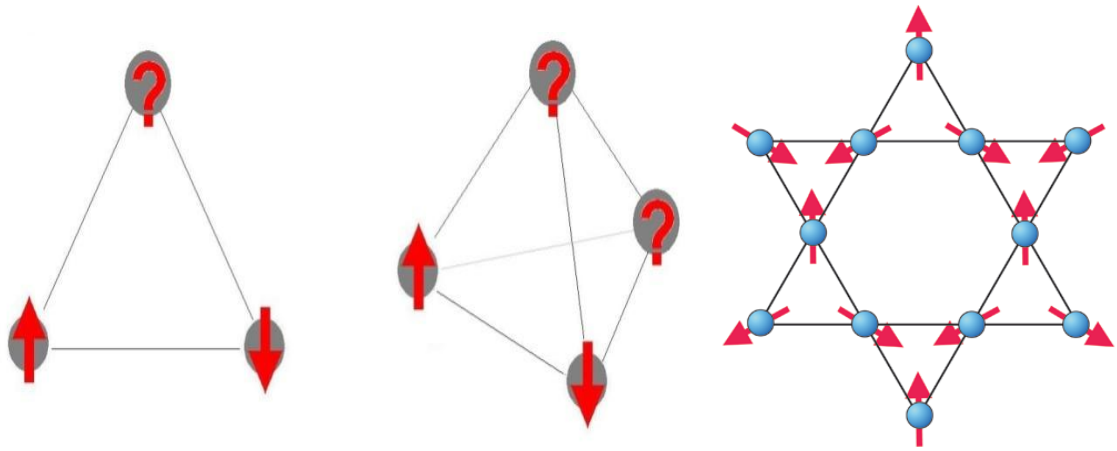

(a) (b) (c)

Fig 1.4: Spin frustration in (a) triangle (b) tetrahedral (c) Kagome lattice.

Degree of frustration can be estimated by relation $f = \Theta_{cw}/T_N$, where Θ_{cw} is the Curie-Weiss temperature and T_N is the Nèel temperature. If the ratio is less than5 the system is less frustrated and if the ratio is more than 5 the system is more frustrated.

1.5. MULTIFERROICS

Multiferroics are a class of materials in which at least two or more of the ferroic orders, namely ferroelectric, ferromagnetic and ferroelastic co-exist.Also multiferroics can defined as the materials which have both spontaneous magnetic and electrical ordering Simultaneously. Also to understand multiferroics we have to understand the ferroic orders.

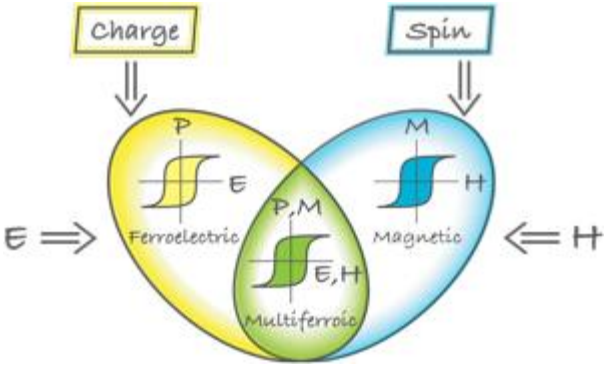

Fig 1.5(a) - Blue circle displays the hysteresis of ferromagnetic materials, yellow circle displays usual hysteresis of ferroelectric materials and the circle displays hysteresis of multiferroics where magneto coupling occurs.**[**D. Khomskii, Phys. 77, 50937 (2009)]

Examples: $BiFeO_3$, $BiMnO_3$, $Bi_2Fe_4O_9$.

Applications of multiferroics:

Multiferroics are used in spintronic devices such as tunnel magneto resistance. In multiferroic thin films the coupling between magnetic and ferroelectric order parameters used for developing magnetoelectric devices. Multiferroic composites in bulk form are used for high sensitivity ac magnetic field sensors. These are also used in electrically tunable microwave devices such as filters, oscillators and phase shifters.

MAGNETOELECTRIC EFFECT

The magneto electric effect was first postulated by Pierre Curie in the nineteenth century. In 1959, Dzyaloshinskii predicted this effect in Cr_2O_3 based on symmetry considerations and Asrov confirmed this prediction experimentally in 1960. Magnetoelectric coupling means the influence of magnetic field on the polarization or the Influence of electric field on magnetization of a material. The effect can be linear or non-linear depending on external fields. This effect also depends upon temperature. This can be represented as

$$P_i=\sum\alpha_{ij}H_j+\sum\beta_{ijk}H_jH_k+\cdots\cdots$$

$$P_i=\sum\alpha_{ij}E_j+\sum\beta_{ijk}E_jE_k+\cdots\cdots$$

Where P=electrictric polarization, M=magnetization, E=electric field, H=magnetic field.α, β are the linear and nonlinear magnetoelectric susceptibilities.

However, due to the weakness of the magnetoelectric coupling in most materials and the consequent difficulties of using it in applications, the research activities in this field went into decline for about two decades. The revival of interest in magnetoelectric materials was initiated by the theoretical investigation of N.Hill in 2000 and by the recent discoveries of new mechanisms of ferroelectricity in perovskite $TbMnO_3$, hexagonal $YMnO_3$.It was also promoted by the recent developments in thin film growth techniques and in experimental methods for observing magnetic and electronic domains.

CLASSIFICATION OF MULTIFERROICS

(A)TYPE-I MULTIFERROICS

Type-I multiferroics are older but till now these are good ferroelectrics, weak coupling of ferroelectricity and magnetism. They have large polarization. The critical temperature of the magnetic and ferroelectric transitions can be well above roomtemperature. Depending on the mechanism of ferroelectricity we can divide them into four subclasses.

Multiferroicperovskites

For multiferroic the coupling between magnetism and ferroelectric is necessary. For magnetism one needs partially filled d shells of a transition metal but in case of ferroelectric perovskites it contains transition metal ions with an empty d shell. In these systems ferroelectricity caused by the off-centre shifts of the transition metal ion, it forms strong covalent bonds with oxygen's using their empty d shells. Now consider magnetic perovskites in which magnetism occurs due to the presence of real d electrons in'd^n' configurations of

magnetic transition metals. These processes prevent ferroelectricity in their perovskites. This is called 'd^0 vs.d^n problem' for which there so rare multiferroics. We can solve this problem by making mixed perovskites with 'd^0' and 'd^n' ions.

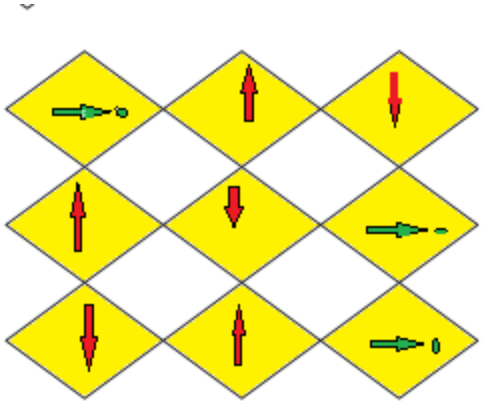

Fig. 1.5(b)-Green circles are ferroelectrically active d^0 ions and red are magnetic d^n ions, yellow plaquettes are shifts of d^0 ions from the centres of O_6 octahedral, green arrows are polarization and red arrows are magnetic order.

Examples: Perovskites $BaTiO_3$, $Pb(ZrTi)O_3$.

It has partially filled d shells for magnetism and empty d shells for ferroelectricity. Transition metal ion is shifted for making covalent bond with O which is in empty d state.

Ferroelectricity due to lone pairs

The electrons which do not participate in chemical bonds are known as lone pairs. They have a high polarizability which is the required condition for ferroelectricity. In $BiFeO_3$, $BiMnO_3$ and $PbVO_3$, Bi^{3+} and Pb^{2+} play in the origin of ferroelectricity. In these ions, there are two outer 6s electrons which act as lone pairs. By ordering of these lone pairs in one direction we can explain the origin of ferroelectricity.

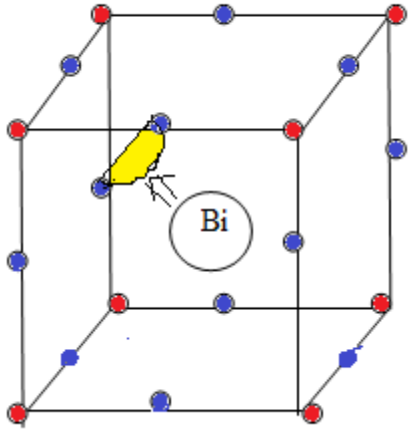

Fig 1.5(c)- In $BiFeO_3$ the ordering of lone pair (yellow lobe) of Bi^{3+} contributes the polarization (arrow).

Ferroelectricity due to charge ordering

This mechanism often observed in transition metal compounds especially in those which contains transition metal ions with different valence. If after charge ordering, both sites and bonds turn out to be in equivalent, this can lead to ferroelectricity. Sometimes we meet the situation in which there are ions with different charge but on the top of that there occurs dimerization. The newly discovered multiferroic Ca_3CoMnO_6 belongs to this class. There is also another way in that is when the bonds are in equivalent because of the structure of the material.

Geometric ferroelectricity

Let's consider an example $YMnO_3$.In this compound ferroelectricity causes by the tilting of the practically rigid MnO_5 block. This tilting occurs to provide closer packing as a result the oxygen ions move closer to the small Y ions. Ferroelectricity does not affect the magnetic Mn^{3+}.

(B)TYPE-II MULTIFERROICS

Type II multiferroics are considered as new type of multiferroics where there is strong drgree of coupling present between electric and magnetic order parameter. The only problem with this class of multiferroics is that the magnitude of electric polarization is very small. . $TbMnO_3$ is one of the most important members of this class of compounds.In this compound at T_{N1}=41 K magnetic ordering appears and at low temperature T_{N2}=28 K the magnetic structure changes. The compound $TbMnO_3$ showed that a magnetic field can strongly influence the electric polarization.By looking the mechanism of multiferroic behaviour we can divide type-II multiferroics into two groups.

Spiral type-II multiferroics

The multiferroics in which ferroelectricity caused by a particular type of magnetic spiral is known as spiral type-II multiferroics .Let's consider an example $TbMnO_3$ .In this compound below T_{N1}=41 K the magnetic structure is a sinusoidal spin-density wave in which all spins point in one direction. This is in antiferromagnetic phase because the total moment for the magnet is zero. Below temperature T_{N2}=28 K the magnetic structure is a cycloidal spin density wave. Here we get nonzero polarization. Kastura, Nagaosa and Balatsky approached a relation for polarization " $\vec{P}$ " in a cycloidal spiral which is given by

$$\vec{P} \approx \vec{r}_{ij} \times \left[\vec{S}_i \times \vec{S}_j\right] \approx \vec{Q} \times \vec{e} \text{ .....} \quad (1)$$

Where $\vec{r}_{ij}$ = vector connecting spins $\vec{S}_i$ and $\vec{S}_j$

$\vec{Q}$ = the wave vector describing the

$\vec{e}$ = spin rotation axis

We found these types of multiferroics basically in magnetic frustration system. This type of multiferroics has also another type of spin structure that is proper-screw spin density wave in which the spins rotate in a plane perpendicular to $\vec{Q}$. It has zero polarization with broken the inversion symmetry.

Type-II multiferroics with collinear magnetic structure

In this type of multiferroicsferroelectricity appears in collinear magnetic structures in which all magnetic moments aligned along a particular axis. In this type magnetic coupling varies with the atomic positions. An example is Ca_3CoMnO_6.It consists of one dimensional chains of alternating Co^{2+} and Mn^{4+} ions .At high temperature the distance between the ions which are in chain are same also the chain has inversion symmetry and polarization is absent. But magnetic ordering breaks the inversion symmetry, it forms ferro and antiferro bonds together but exchange striction differentiates the ferro and antiferro bonds as a result at the end the material becomes ferroelectric.

There is another mechanism which gives ferroelectricity in a collinear magnet is the electronic ferroelectricity in frustrated magnets. Here the polarization of spins of a triangle is proportional to the spin correlation function $\vec{S}_1\left(\vec{S}_2+\vec{S}_3\right)-2\vec{S}_2\vec{S}_3$.Here 1, 2,3 denotes the vertices of the triangle.

SPIN CURRENT MODEL

This model was proposed by Kasura*et al.* The mechanism of magnetically induced ferroelectricity in spin spiral structures has been studied using microscopic and phenomenological approaches.

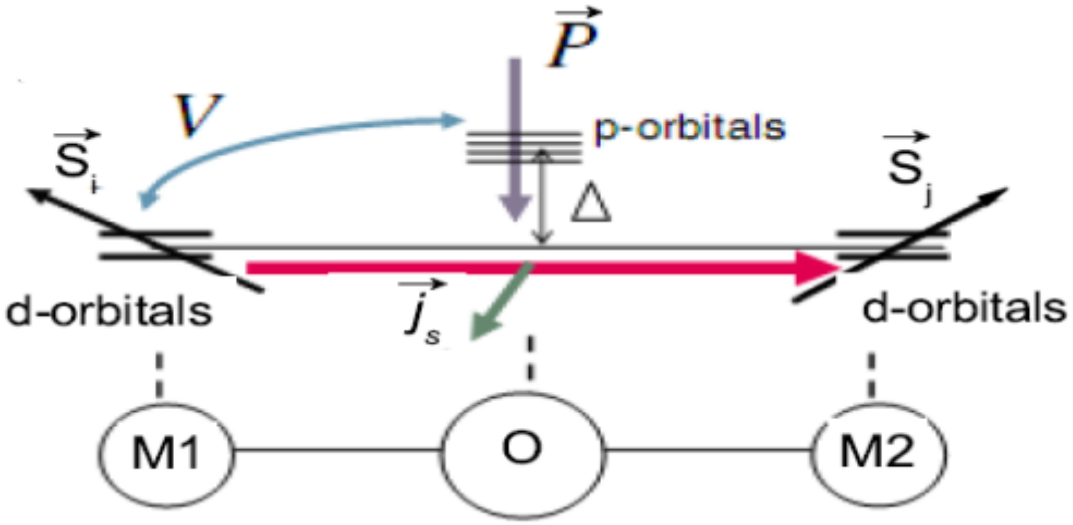

(d)

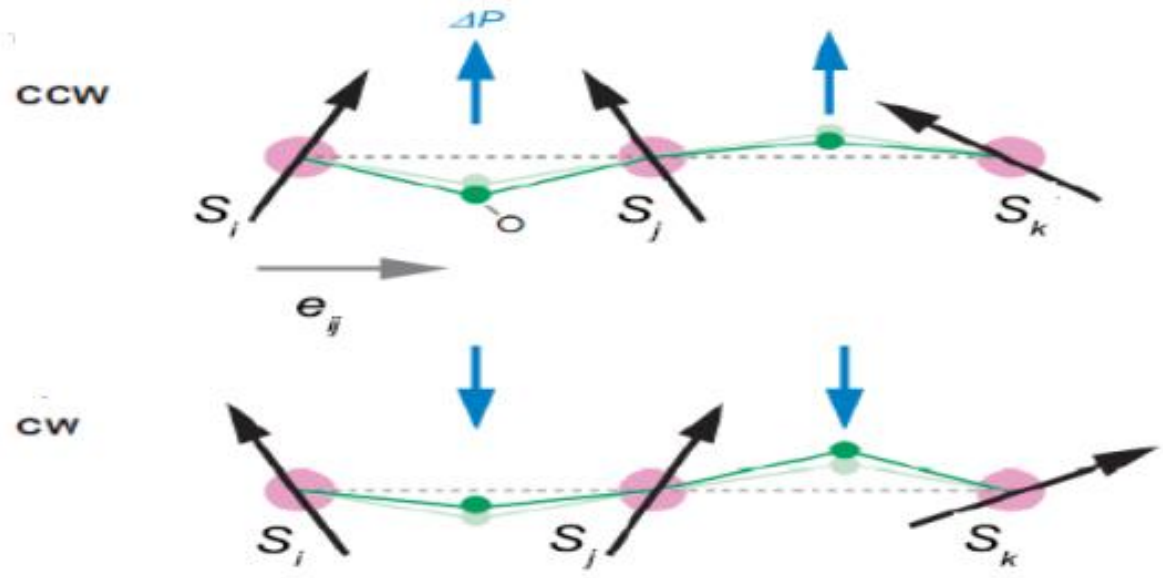

(e)

Fig- 1.5(d) Microscopic mechanism of spin-induced polarization for the spin current model of Katsura et al. Schematics pictures of the change of local electric polarization induced by spin canting **(e)** counter clockwise and (clockwise) spiral structures.[Phys. Rev. Lett.95, 057205 (2005).]

The microscopic mechanism considers a spin current that arises in the presence of two coupled no collinear spins $(\vec{J}_s \propto \vec{S}_1 \times \vec{S}_2)$. A polarization is induced that is proportional to the vector product of the spin current and the unit vector $\vec{e}_{12}$ that connects the two magnetic ions: $\vec{P} \propto \gamma(\vec{e}_{12} \times \vec{J}_S)$. This effect can also be described in terms of an inverse Dzyoloshinskii-Moriya (DM) interaction, proposed by Sergienko*et al.* In this model, two non-collinearly coupled magnetic moments displace the oxygen atom located between them via an electron-lattice interaction. In the spiral structure the displacement of the oxygen ion is always in the same direction because the vector product of S_n and S_{n+1} has the same sign for all pairs of neighbouring spins. When the exchange between two spins is reversed, the sign of the effect in the asymmetric DM interaction is also reversed $(\vec{S}_i \times \vec{S}_j) = (\vec{S}_j \times \vec{S}_i)$, hence the sign of the electric polarization can be switched by a reversal of the spin spiral.

2. MOTIVATION

Generally from crystallography we know pentagon symmetry does not exist but $Bi_2Fe_4O_9$ shows pentagon symmetry which is unique. $Bi_2Fe_4O_9$is a type II multiferroic for which it is very easy to control electrical polarization using magnetic field. For most of the multiferroics the transition temperature is below liquid nitrogen temperature but $Bi_2Fe_4O_9$provides an opportunity to study magnetoelectric coupling very near to room temperature (265 K). The present thesis explores the effect of Co doping at Fe site which is not well studied before.

3.1.CRYSTAL STRUCTURE OF $Bi_2Fe_4O_9$

High resolution X-ray diffraction shows that $Bi_2Fe_4O_9$ has orthorhombic structure with space group *Pbam*. The lattice constants of this structure are a=7.965Å,b=8.440Å,c=5.994Å.The iron ions in the $Bi_2Fe_4O_9$ lattice are evenly distributed between the tetrahedral and octahedral positions with the bismuth ions surrounded by eight oxygen atoms.

3.2. MAGNETIC STRUCTURE OF $Bi_2Fe_4O_9$

The magnetic structure of this compound can be analysed by neutron diffraction method. This compound belongs to the space group pbam. The neutron diffraction measurement showed that it is paramagnetic at room temperature and undergoes to an phase transition to an antiferromagnetic state at T_N=264 K. The magnetic moment of the compound was found to be (4.95 ± 0.08) μ_B. Analysis of the 80 K neutron diffraction pattern introduced a magnetic structure with some features that are the basic translations a_0, b_0, c_0 of the chemical lattice change into antitranslations in the magnetic lattice. The spins are perpendicular to c_0.

As shown in the figure 3.2 there are four octahedral Fe ions on the sides of the cell and the remaining four tetrahedral Fe ions are in the interior. By the super-exchange route tetrahedral Fe spins interact antiferromagnetically among themselves and with the octahedral Fe spins while there is a ferromagnetic coupling within a pair of octahedral spins. These competing exchange interactions generate spin frustration in this system.

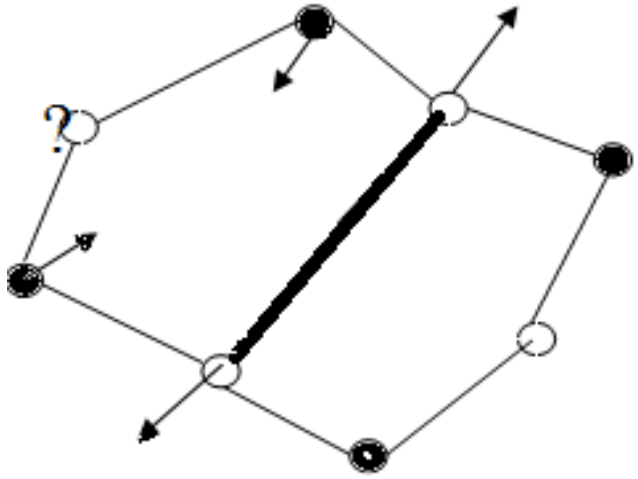

Fig.3.2-Spin frustration in $Bi_2Fe_4O_9$

4. PREVIOUS REPORTS

4.1. Phonon and magnon scattering of antiferromagnetic Bi_2Fe_4O9 , By M. N. Iliev, A. P. Litvinchuk, and V. G. Hadjiev, Phys Rev B.81.024302 (2010)

The phonon structure of antiferromagnetic $Bi_2Fe_4O_9$ was studied by the authors theoretically by calculations of lattice dynamics and experimentally between 10 and 300 K by polarized Raman spectroscopy. Most of the $12A_g+12B_{1g}+9B_{2g}+9B_{3g}$ Raman modes were unambiguously identified. Strong second-order scattering was observed for ab-plane confined incident and scattered light polarizations. In addition to the phonon scattering, typical characteristics of magnon scattering of broad Ramam bands appear below $T_{N.}$ The magnon bands are analyzed on the basis of magnetic structure of the compound and attributed to two magnon excitations**.**

4.2.Substantial magneto-electric coupling near room temperature in $Bi_2Fe_4O_9$, by A. K. Singh, S. D. Kaushik, Brijesh Kumar and S. Patnaik [Appl. Phys. Lett. 92 132910 (2008)]

The authors reported a remarkable multiferroic effects in polycrystalline $Bi_2Fe_4O_9$. High resolution X-ray diffraction they found that the compound has orthorhombic structure. Magnetic measurements confirmed an antiferromagnetic transition around ~265 K and a pronounced inverse S-shape anomaly in the loss tangent of dielectric measurement observed near Nèel temperature. This feature shifts with the application of magnetic field. From these anomalies they indicated that substantial coupling between the electric and magnetic orders occurs in that compound.

5. SAMPLE PREPARATION

5.1. SYNTHESIS OF $Bi_2Fe_4O_9$

- 2 gm of $Bi_2Fe_4O_9$ is prepared through solid state reaction route using 1.1866 g of Bi_2O_3 and 0.8133 g of Fe_2O_3.
- It follows the reaction:

$$Bi_2O_3 + 2Fe_2O_3 \rightarrow Bi_2Fe_4O_9$$

- Bi_2O_3 and Fe_2O_3 in 1:2 molar ratio is taken and mixed by grinding for 3 hours.
- Calculation

  Atomic weight of

  Bi = 208.98

  O = 15.99

  Fe = 55.84

  Molecular weight of

  $Bi_2O_3 = (2 \times 208.98) + (3 \times 15.99)g$

$= 417.96 + 47.97 = 465.959\ g$

$Fe_2O_3 = (2 \times 55.84) + (3 \times 15.99)g = 111.8 + 47.97g$

$= 159.688g$

$Bi_2Fe_4O_9 = (2 \times 208.98) + (4 \times 55.84) + (9 \times 15.99)g$

$= 417.96 + 223.36 + 143.91g$

$=785.335g$

For 2 g of $Bi_2Fe_4O_9$ required weight of

$Bi_2O_3 = (465.959 \div 785.3354) \times 2g$

$= 1.1866\ g$

$Fe_2O_3 = \{(159.688 \times 2) \div 785.335\} \times 2g$

$= 0.8133\ g$

5.2. SYNTHESIS OF $Bi_2Fe_{3.5}Co_{0.5}O_9$

- 2 g of $Bi_2Fe_{3.5}Co_{0.5}O_9$ is also prepared through solid state reaction route using 1.1843 g of Bi_2O_3, 0.7102 g of Fe_2O_3 and 0.1020 g of Co_3O_4.
- It follows the reaction:

$$Bi_2O_3 + 1.75Fe_2O_3 + 1.67\ Co_3O_4 \rightarrow Bi_2Fe_{3.5}Co_{0.5}O_9$$

- The mixture is mixed by grinding for 3 hours.
- Calculation

Atomic weight of Co = $58.93\ g$

Molecular weight of$Co_3O_4 = (3 \times 58.93) + (4 \times 15.99)g$

$$= 176.79 + 63.96g = 240.797\ g$$

$Bi_2Fe_{3.5}Co_{0.5}O_9 = (2 \times 208.98) + (3.5 \times 55.84) + (0.5 \times 58.93) + (9 \times 15.99)\ g$

$= 417.96 + 195.44 + 143.91\ g = 786.879\ g$

For 2 g of $Bi_2Fe_{3.5}Co_{0.5}O_9$ required weight of

$Bi_2O_3 = (465.959 \div 786.879) \times 2g = 1.1843\ g$

$Fe_2O_3 = \{(159.688 \times 1.75) \div 786.879\} = 0.7102\ g$

$Co_3O_4 = \{(240.797 \times 0.1667) \div 786.879\} \times 2g = 0.1020\ g$

PRESSING

Before making pallets, all the samples were ground in alumina mortar pestle for three hours in order to maintain homogeneity. The powders were pressed using stainless die of diameter 10mm. The pressure was applied to the powder sample using Hydrolytic press. The thicknesses of the final sintered pallets were ~ 1mm. The applied pressure for making pallets was ~ 5 ton.

SINTERING

All pellets were kept into the furnace and sintered at 850 ˚C for 12 hours. The ramping rate for cooling and heating was kept at 5˚ C/min. Then after first sintering the pellets were broke, again ground for half an hour and again pellets were made. Then kept in furnace for second sintering at 850˚C for 12 hours keeping heating rate same.

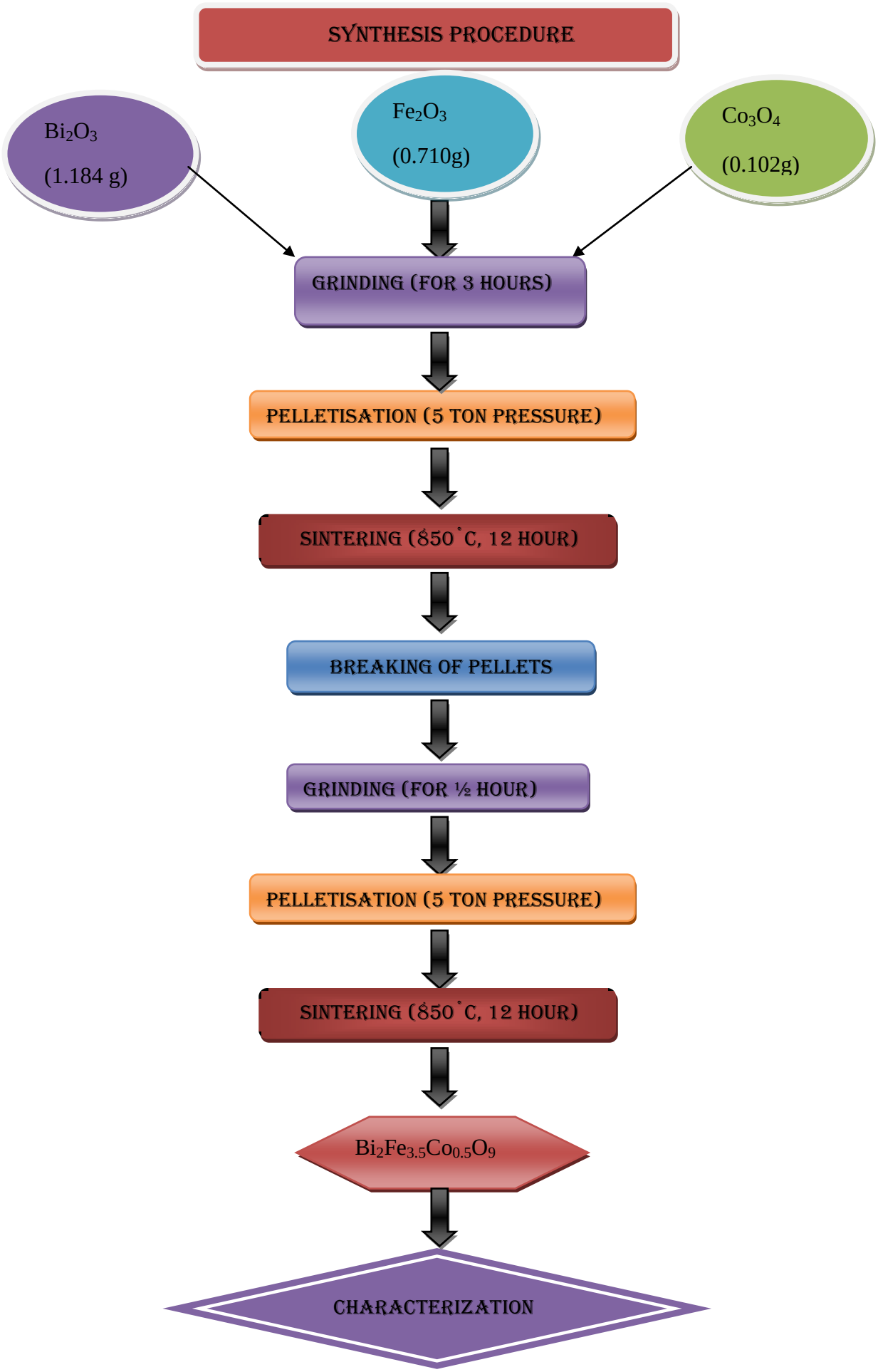

Fig.5-Flow chart for steps followed in sample preparation

6. CHARACTERISATION TECHNIQUES

6.1. X-RAY DIFFRACTION

X-ray diffraction is based on constructive interference of monochromatic X-rays and a crystalline sample. It is used for determining the arrangement of atoms within a crystal in which a beam of x-rays strikes a crystal and causes beam to spread into many specific directions. These X-rays are generated by a cathode ray tube, which filtered to produce monochromatic radiation, collimated to concentrate, and directed toward the sample.

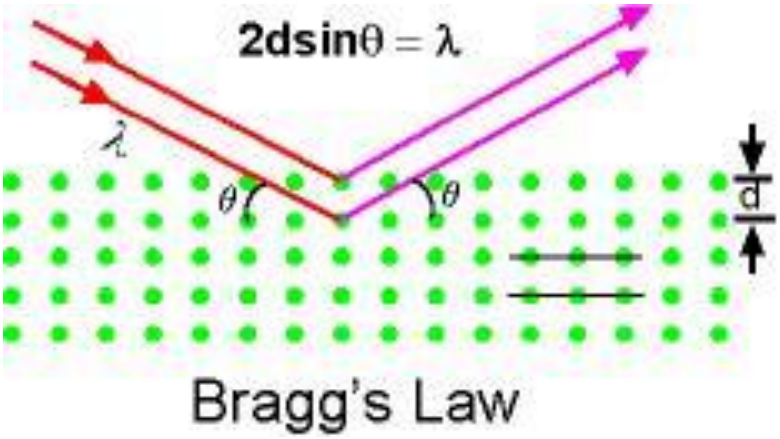

Fig 6.1– Bragg's diffraction condition.

The interaction of the incident rays with the sample produces constructive interference (and a diffracted ray) when conditions satisfy ***Bragg's Law*** ($n\lambda=2d \sin\theta$). By scanning the sample through a range of 2θ angles, all possible diffraction directions of the lattice should be attained due to the random orientation of the powdered material. All diffraction methods are based on ***generation of X-rays*** in an X-ray tube. These X-rays are directed at the sample, and the diffracted rays are collected. A key component of all diffraction is the angle between the incident and diffracted rays. Accordingly, phenomena like constructive and destructive interference should become observable when crystalline and molecular structures are exposed to x-rays.

In the X-ray diffraction methods, the scattering is elastic; the scattered X-rays have the same wavelength as the incoming X-ray. In X-ray diffraction work we normally distinguish between single crystal and polycrystalline or powder applications. The single crystal sample is a perfect (all unit cells aligned in a perfect extended pattern) crystal with a cross section of about 0.3 mm. In powder or polycrystalline diffraction it is important to have a sample with a smooth plane surface. The sample is homogeneous and the crystallites are randomly distributed. The sample is pressed into a sample holder so that we have a smooth flat surface.

6.2. SCANING ELECTRON MICROSCOPY

The scanning electron microscope (SEM) uses a focused beam of high-energy electrons to generate a variety of signals at the surface of solid specimens. The signals derived from electron-sample interactions, it gives information about the sample including external morphology, chemical composition, and crystalline structure and orientation of materials making up the sample. In most applications, data are collected over a selected area of the surface of the sample, and a 2-dimensional image is generated that displays spatial variations in these properties. Areas ranging from approximately 1 cm to 5 microns in width can be imaged in a scanning mode using conventional SEM techniques. The SEM is also capable of performing analyses of selected point locations on the sample; this approach is especially useful in qualitatively or semi-quantitatively determining chemical compositions, crystalline structure, and crystal orientations.

Fundamental Principles of Scanning Electron Microscopy

(a)Electron gun

They produce the steady stream of electrons necessary for SEM to operate. Electron guns are typically one of two types.Thermionic guns which apply thermal energy to a filament to coax electrons away from the gun and toward the specimen under

examination**.** Fieldemission guns create a strong electrical field to pull electrons away from the atoms they're associated with. The location of electron guns is either at the top or at the bottom of an SEM and fire a beam of electrons at the object under examination.

(b)Lenses

SEMs use lenses to produce clear and detailed images. The lenses in these devices, work differently. The lenses are made of magnets capable of bending the path of electrons. By doing so, the lenses focus and control the electron beam, ensuring that the electrons end up precisely where they need to go.

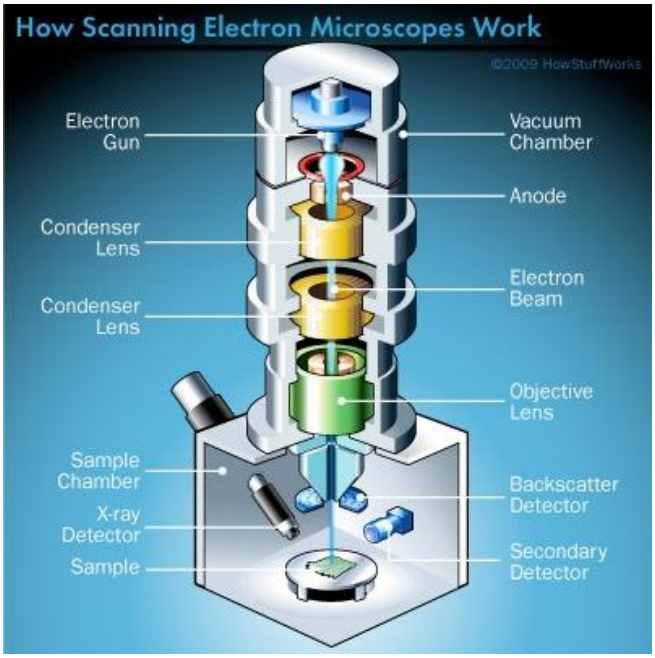

Fig. 6.2 - Schematics of SEM.(www.google.com)

(c)Sample chamber

The sample chamber of an SEM is where the samples are placedfor examining. Because the specimen must be kept extremely still for the microscope to produce clear images, the sample chamber must be very sturdy and insulated from vibration. The sample chambers of an SEM do more than keep a specimen still. They also manipulate the specimen,

placing it at different angles and moving it so that researchers don't have to constantly remount the object to take different images.

(d)Detectors

These devices detect the various ways that the electron beam interacts with the sample object. Everhart-Thornley detectors register secondary electrons, which are electrons dislodged from the outer surface of a specimen. The detectors are capable of producing the most detailed images of surface of an object. Other detectors, such as backscattered electron detectors and X-ray detectors, can tell about the composition of a substance.

(e)Vacuum chamber

SEMs require vacuum for operation. Without vacuum, generated electron beam by the electron gun would encounter constant interference from air particles in the atmosphere. Not only would these particles block the path of the electron beam, they would also be knocked out of the air and onto the specimen, which would distort the surface of the specimen.

6.3. DIELECTRIC SPECTROSCOPY

Dielectric spectroscopy measures the dielectric property of a sample as a function of frequency. The basic principle is based on the interaction of an external field with the electric dipole moment of the sample, expressed by permittivity. This technique measures the impendence of a sample over a range of frequencies, and therefore the frequency response of the system, also it includes the energy storage and dissipation properties.

Tangent loss (tanδ) of a dielectric material quantifies its inherent dissipation of electromagnetic energy. It is the tangent of the angle between the lossy component of an

electromagnetic field and its lossless component.Dielectrics are used to mechanically support electrical conductors and keep them at a fixed separation, or to provide a barrier between different gas pressures yet still transmit electromagnetic power. Maxwell's equations are solved for the electric and magnetic field components of the propagating waves that satisfy the boundary conditions of geometry of the specific environment. In such electromagnetic analyses, the parameters permittivityϵ, permeability μ, and conductivity σ represent the properties of the media through which the waves propagate. The permittivity can have real and imaginary components such that

$$\epsilon = \epsilon' - j\epsilon''$$

If we assume that we have a wave function such that

$$E = E_0 \, e^{jwt}$$

Then Maxwell's curl equation for the magnetic field can be written as

$$\nabla \times H = jw\epsilon' E + \left(w\epsilon'' + \sigma\right)E$$

Where $\epsilon''$is the imaginary amplitude of permittivity, which gives rise to energy loss. The component ϵ'represents the familiar lossless permittivity. The loss tangent is then defined as the ratio of the lossy reaction to the electric field E in the curl equation to the lossless reaction:$tan\delta = \frac{w\epsilon'' + \sigma}{w\epsilon'}$

For most dielectrics with small loss, this angle is $\ll 1$ and tan $\delta \approx \delta$.

6.4. UV-VIS SPECTROSCOPY

Spectroscopy basically means the study of the interaction between radiation and matter as a function of wavelength (λ). Historically, spectroscopy referred to the use of visible light dispersed according to its wavelength. Dispersion of different wavelengths is accomplished with the separating capability of fraction (prism) or diffraction (diffraction grating). Typical applications are isolation of a narrow band of radiation from a continuum light source for absorption measurements, or analysis of the emission from excited atoms or

molecules. Later the concept was expanded greatly to comprise any measurement of a quantity as a function of either wavelength or frequency. Thus, it can refer to a response to an alternating field or varying frequency (v). A further extension of the scope of the definition added energy (E) as a variable, once the very close relationship $E = hv$ for photons was realized (h is the Planck constant). UV Visible spectroscopy measures the response of a sample to ultraviolet and visible range of electromagnetic radiation. All molecules and atoms have electronic transitions while most of the solids have interband transitions in the UV and Visible range. Most molecules have a π to π^* transition.

7. RESULTS AND DISCUSSION

7.1. X-RAY ANALYSIS

In x-ray diffraction, the samples are scanned in a continuous mode from 20˚-80˚ with a scanning rate of 2˚ per minute. XRD pattern of pure $Bi_2Fe_4O_9$ sintered at 850˚c is shown in the figure 7.1(a). The prominent peaks in the plot are indexed to various [hkl] planes of $Bi_2Fe_4O_9$ using JCPDFWIN. Besides these peaks there are some low intensity peaks which are not matched with $Bi_2Fe_4O_9$ peaks, marked as *. These are impurity peaks; it may be due to iron oxide (Fe_2O_3) and bismuth oxide (Bi_2O_3).

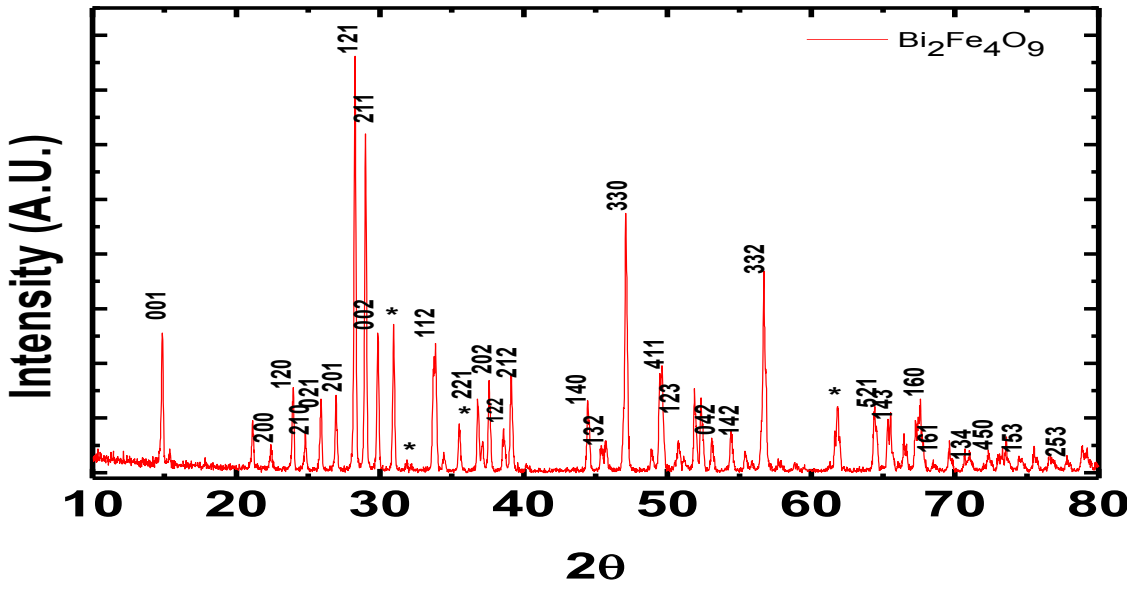

Fig. 7.1(a) - XRD plot of $Bi_2Fe_4O_9$.

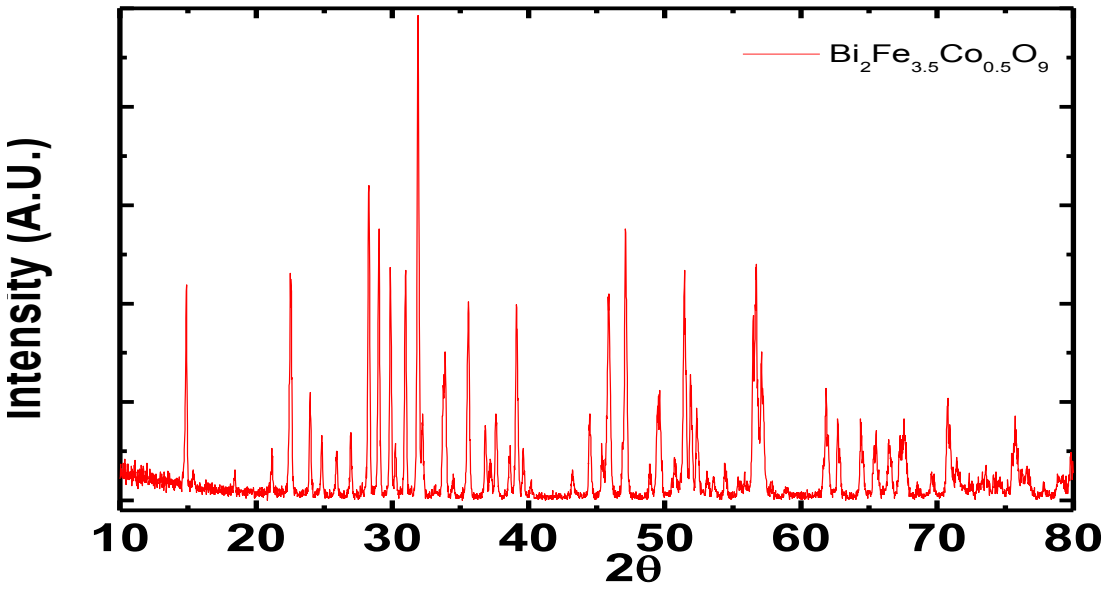

Fig. 7.1(b) - XRD plot of 10% Co-doped $Bi_2Fe_4O_9$.

From literature survey I know the value of lattice parameters a, b, c are 7.965Å, 8.440 Å and 5.994 Å respectively. Here I calculated these parameters by taking three [h k l] values from the XRD plot. We can calculate "d" by using Bragg's diffraction condition $2dsin\theta = n\lambda$. Here n is taken as 1. $Bi_2Fe_4O_9$ has orthorhombic structure. For orthorhombic structures the relation between hkl and a, b, c is given by $\frac{1}{d^2} = \frac{h^2}{a^2} + \frac{k^2}{b^2} + \frac{l^2}{c^2}$. I

have taken (200), (021), and (111) values then by solving this I found the values of a, b, c are 7.96 Å, 9.12 Å, and 5.26 Å respectively.

Figure 7.1(c) shows the x-ray diffraction plot of both $Bi_2Fe_4O_9$ and10% Co-doped $Bi_2Fe_4O_9$ from these we can see that most of major peaks are matched with pure $Bi_2Fe_4O_9$ plot. Besidesthese some other peaks are present which are may be due to reaction with alumina crucible, and also there is a possibility of cobalt loss at high temperatures. I have calculated the crystalline size by using scherrer formula $D = 0.9\ \lambda/\beta\ \cos\theta$ and got the size of crystal 51.26 nm and 51.69 nm for $Bi_2Fe_4O_9$and 10% Co doped $Bi_2Fe_4O_9$respectively. From this I concluded that crystal size increases due to doping.

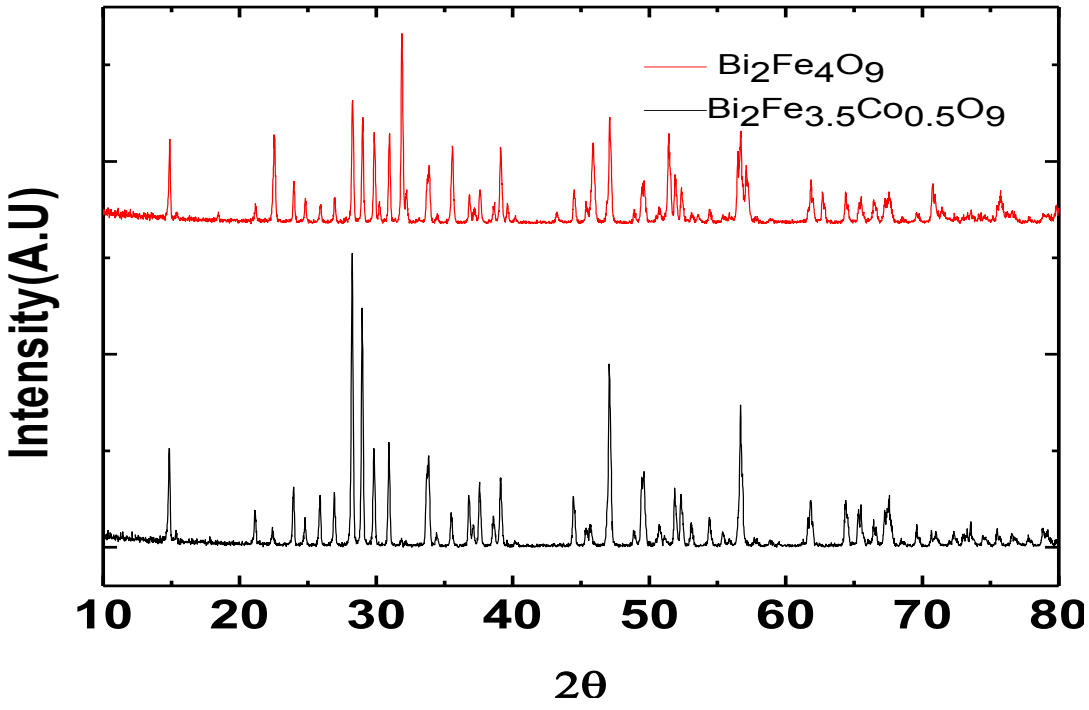

Fig. 7.1(c)-XRD plot of both $Bi_2Fe_4O_9$ and 10% Co doped $Bi_2Fe_4O_9$.

7.2. SEM ANALYSIS

Figure 7.2(a) and 7.2(b) shows the Scanning Electron Microscope (SEM) images of pure $Bi_2Fe_4O_9$ and 10% Co-doped $Bi_2Fe_4O_9$respectively.From fig 7.2 (a), we confirm that grains of $Bi_2Fe_4O_9$are not well separated. The distribution of grains around the whole sample is not uniform. On the other hand, fig 7.2 (b) shows that grains of $Bi_2Fe_{3.5}Co_{0.5}O_9$are well

separated, grain size are uniform as compare to $Bi_2Fe_4O_9$. Thus we confirm that due to 10% Co doping the porosity of the sample increases but the distribution of the grain size becomes uniform.

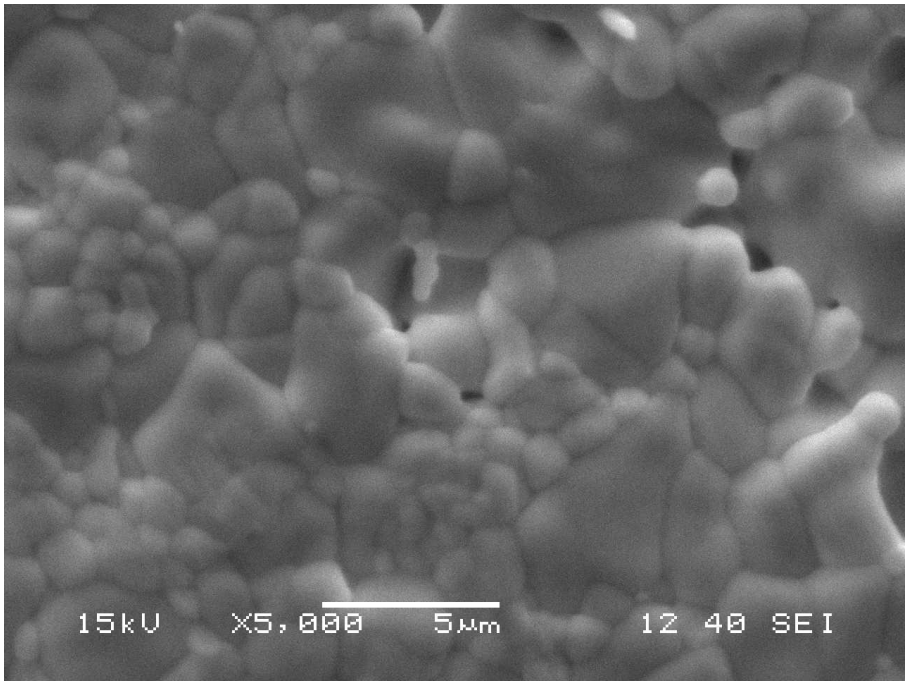

Fig. 7.2(a) SEM image of $Bi_2Fe_4O_9$.

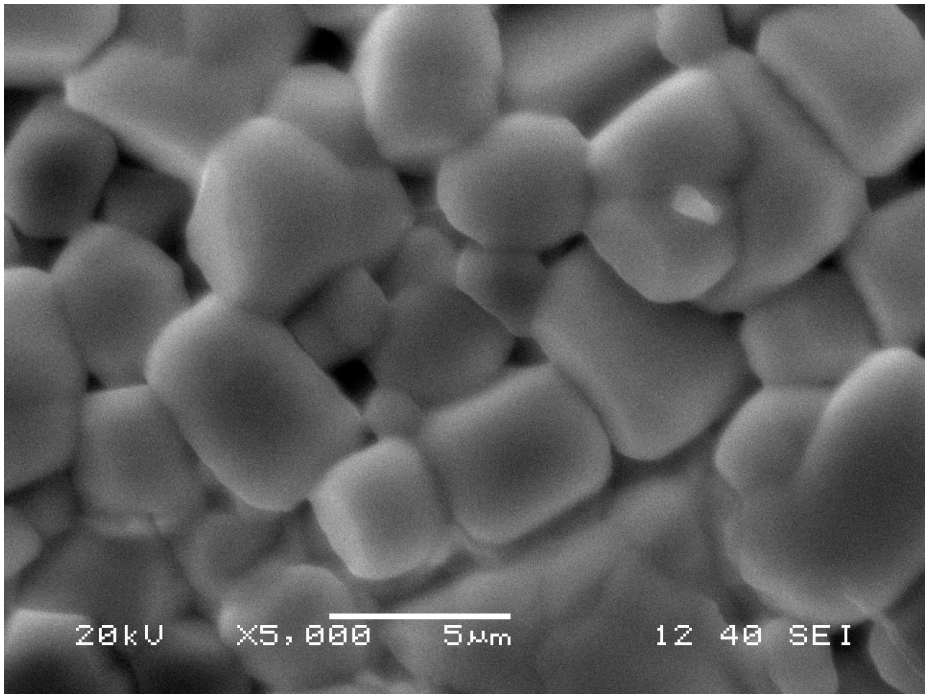

Fig 7.2(b) – SEM image of 10% Co doped $Bi_2Fe_4O_9$.

7.3. DIELECTRIC MEASUREMENT

The dielectric measurement as a function of frequency in the range 100 Hz to 1 MHz is done. Fig 7.3(a), 7.3(b),shows the variation of tan δ with the frequency, variation of impendence with frequency for $Bi_2Fe_4O_9$. We can see from the figure 7.3(a) that tan δ decreases linearly with frequency while in fig 7.3(b)impendence remain constant till frequency reaches 10^4 Hz, then decreases with increasing frequency.

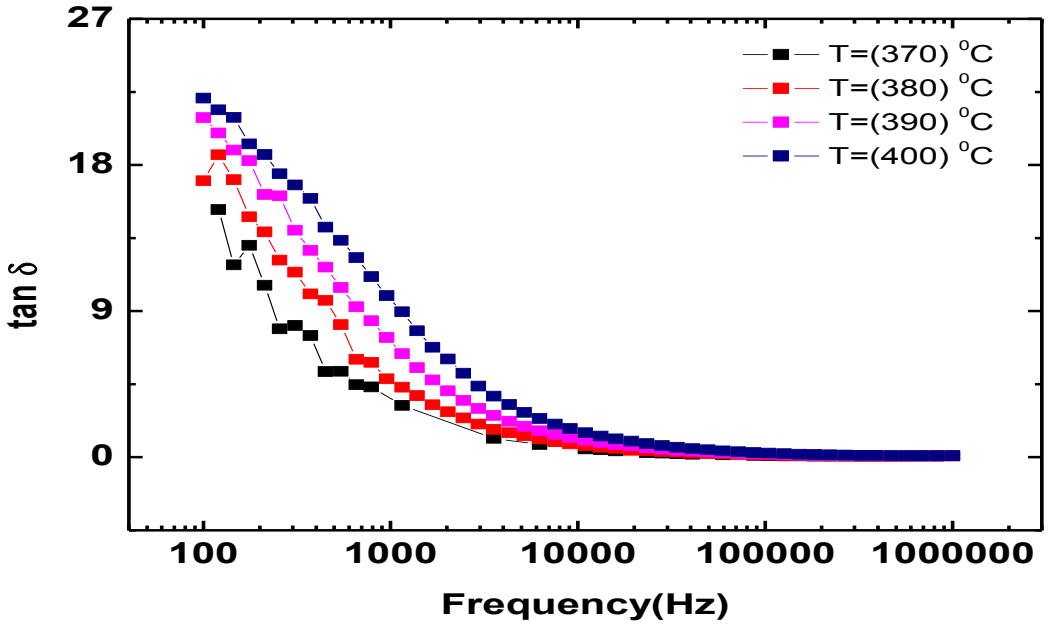

Fig. 7.3(a) -Variation of tan δ with frequencyof $Bi_2Fe_4O_9$

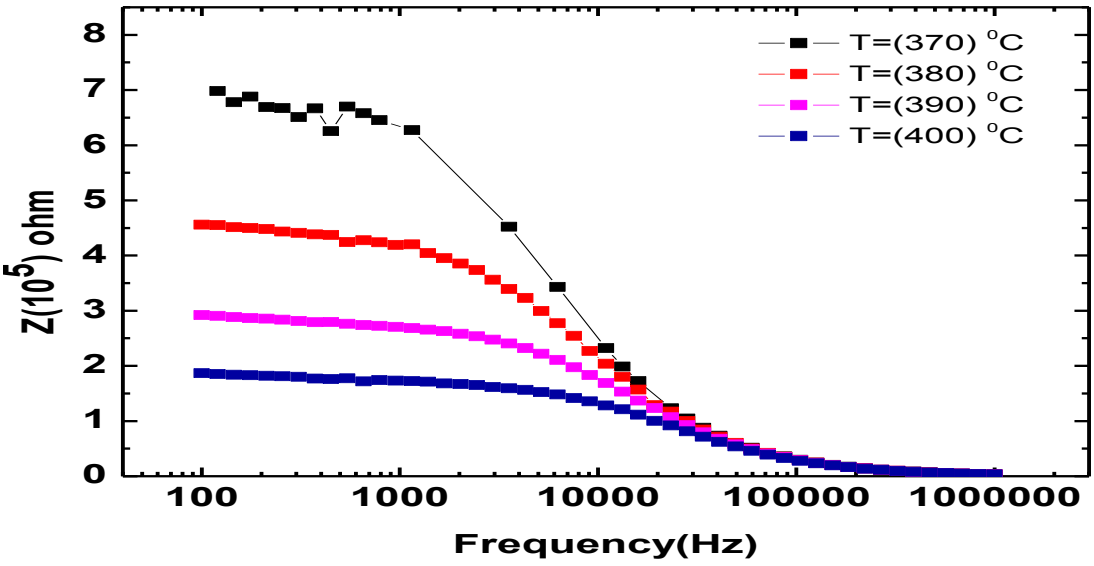

Fig.7.3 (b)- Variation of impendence with frequencyof $Bi_2Fe_4O_9$

Fig 7.3(c), 7.3(d) shows the variation of tan δ with the frequency, variation of impendence with frequency for 10 % Co doped $Bi_2Fe_4O_9$. The result is same as pure $Bi_2Fe_4O_9$. Fig 7.3(e) shows the comparison between variation of dielectric constant in both pure $Bi_2Fe_4O_9$ and doped $Bi_2Fe_4O_9$. From this graph we get the information that 10% Co doped $Bi_2Fe_4O_9$ has high dielectric constant as compare to pure $Bi_2Fe_4O_9$.

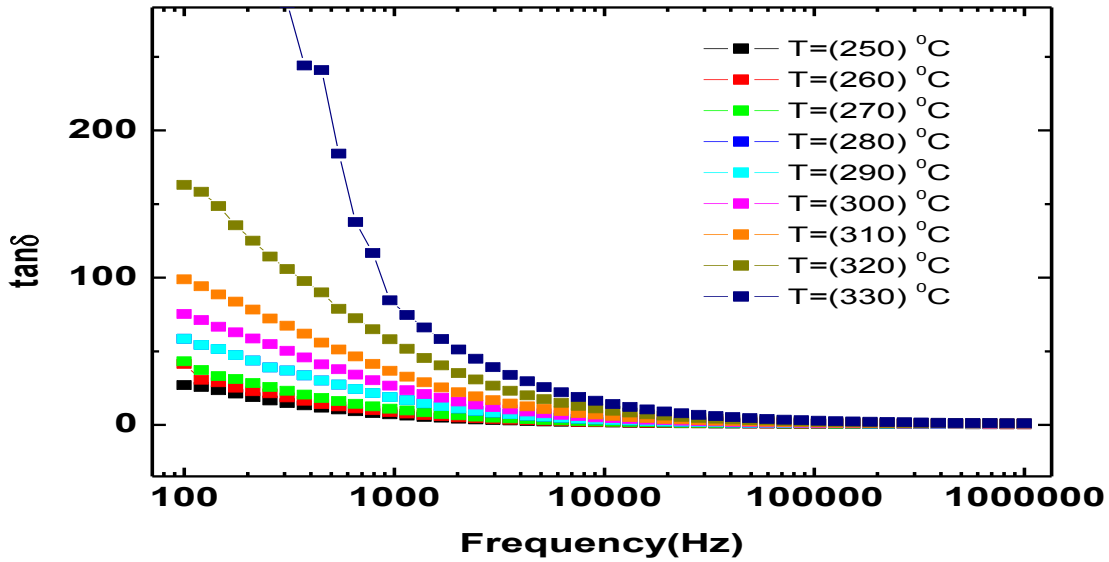

Fig.7.3 (c)-Variation of tan δ with frequency of 10% Co doped $Bi_2Fe_4O_9$.

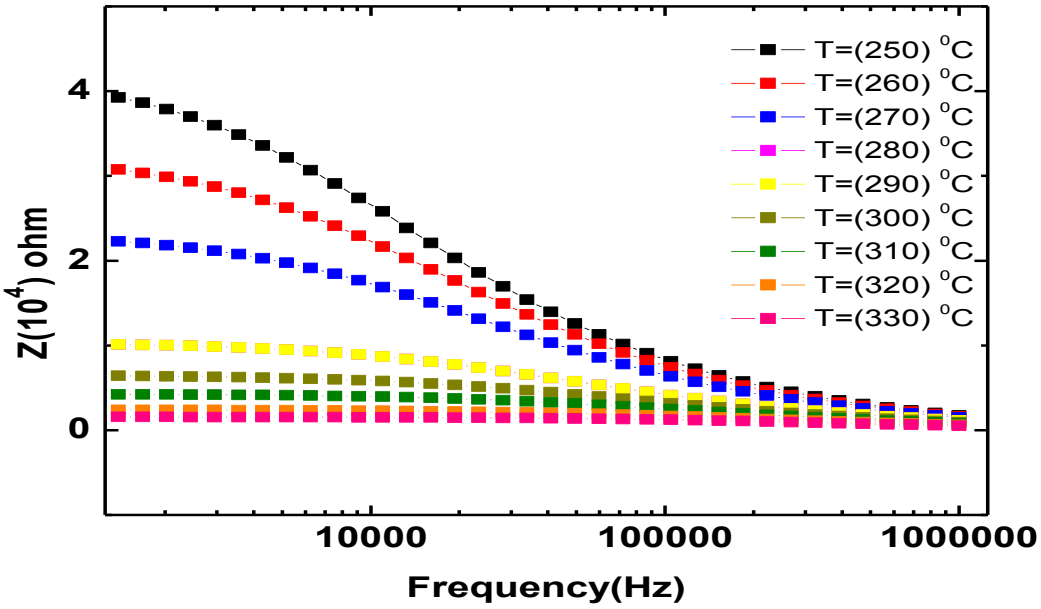

Fig.7.3 (d)-Variation of impendence with frequency of 10% Co doped$Bi_2Fe_4O_9$.

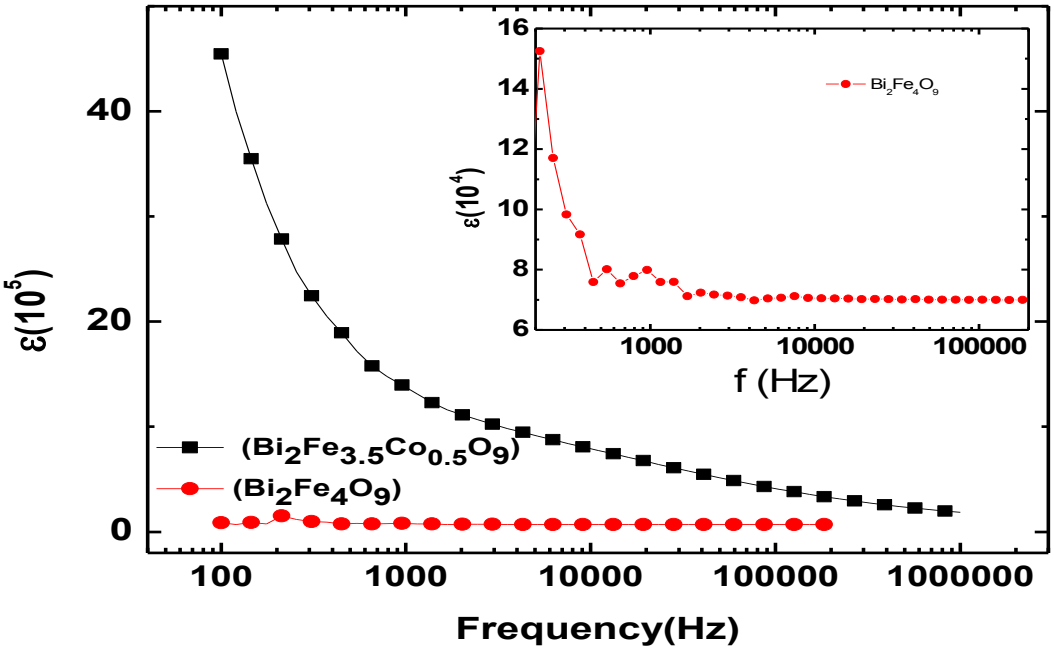

Fig.7.3 (e) -Variation of dielectric constant with frequency in both $Bi_2Fe_4O_9$ and 10% Co doped $Bi_2Fe_4O_9$.

7.4. UV ANALYSIS

Fig. 7.4(a) and fig. 7.4(b) shows the variation of energy with absorption coefficient of pure $Bi_2Fe_4O_9$ and 10% Co doped $Bi_2Fe_4O_9$ respectively. From these graph we can see where the slope touches the energy curve gives the band gap energy i.e. 4.6 for pure $Bi_2Fe_4O_9$ and 4.8 for 10% Co doped $Bi_2Fe_4O_9$. From these we have concluded that band gap energy increases by doping.

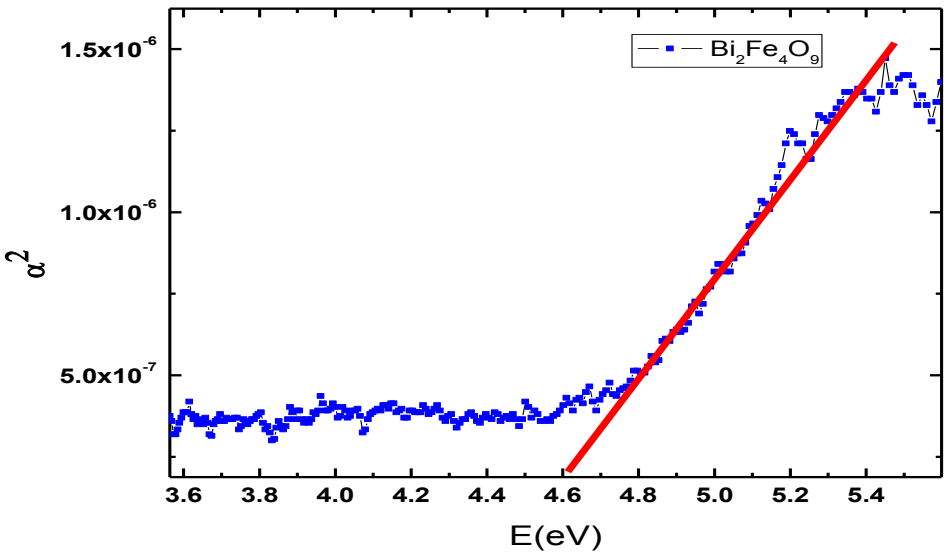

Fig. 7.4(a) – Absorption spectra of $Bi_2Fe_4O_9$.

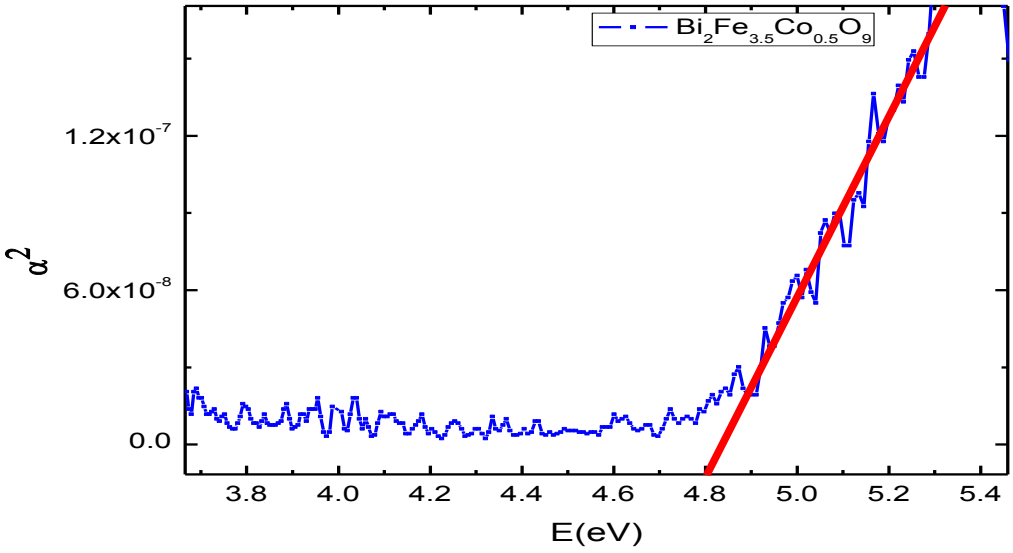

Fig. 7.4(b) – Absorption spectra of Co doped $Bi_2Fe_4O_9$.

8. CONCLUSION

X- ray diffraction analysis shows that due to 10% Co doping crystal structure remains the same. From SEM image, we observe that due to doping the grain size becomes large and uniform as compare to parent $Bi_2Fe_4O_9$. The grain sizes are in accordance with crystallite size calculated from XRD analysis. Dielectric measurement shows that 10% Co doped sample has higher dielectric constant as compare to parent $Bi_2Fe_4O_9$. From UV-visible spectroscopy, we calculated the band gap energy and conclude that band gap energy increases due to doping.

9. REFERENCES

1. Introduction to Solid State Physics, Charles Kittel, Wiley Student's 7th Edition.
2. Spin current and magnetoelectric effect in no collinear magnets, HoshoKatsura, Naoto Nagaosa, Alexander V. Balatsky, and Phys.Rev.Lett. 95, 057205(2005).
3. The renaissance of magnetoelectricmultiferroics, Nicola A. Spaldin and Manfred Fiebig, Science 10, 1114671 (2005).
4. Spiral magnets as magnetoelectrics by T. Kimura, Nicola A. Hill, and J. Phys. Chem. B 104, 6694 (2000)
5. Classifying multiferroics: Mechanisms and effects, D.Khomskii,Phys. 77, 50937 (2009).
6. Magnetic frustration in an iron based Cairo pentagonal lattice, E. Ressouche, V. Simonet, B. Canals, M. Gospodinov and V. Skumryev, Phys.Rev.Lett. 103, 267204(2009)
7. Phonon and magnon scattering of antiferromagnetic Bi_2Fe_4O9, M. N. Iliev, A. P. Litvinchuk, and V. G. Hadjiev, Phys Rev B.81, 024302(2010).
8. Why are there so fewmagnetic ferroelectrics, Nicola A. Hill, J. Phys. Chem. B 104, 6694 (2000).
9. Substantial magnetoelectric coupling near room temperature in $Bi_2Fe_4O_9$, A. K. Singh, S. D. Kausik, Brijesh Kumar and S. Patnaik, Appl. Phy. Lett. 92, 132910(2008).
10. Synthesis and characterization of $Bi_2Fe_4O_9$ powders, Jingyoan Zhao *et al*.Mater. Chem.&Phys. 128, 338 (2011).
11. Tunable morphology of $Bi_2Fe_4O_9$ crystals for photocatalytic oxidation, Qian -Jing Ruan and Wei – De Zhang,J. Phys. Chem. C 113, 4168 (2009).
12. Effect of antiferromagnetic order on the dielectric properties of Bi2Fe4O9, Y. A. Park *et al*, Appl. Phy. Lett, 96, 092506(2010).
13. Enhanced multiferroic properties in Ti – doped $Bi_2Fe_4O_9$ ceramics, Z. M. Tian*et al.*, Appl. Phys. 10,064110(2010).
14. Geometrically frustrated magnetic materials,John E. Greedan, J. Mater.Chem. 11, 37 (2011).